Medicinal
Plant Biology

ARTICLE

Open Access

https://doi.org/10.48130/MPB-2022-0002
Medicinal Plant Biology **2022**, 1:2

Functional characterization of a UDP-xylose-preferring *C*-glycosyltransferase from *Lemna aequinoctialis*

Sharpkate Shaker, Zhi-Min Hu, Zi-Long Wang, Guo Ye, Jin-Chen Long, Xin-Fang Zhai, Xue Qiao*, and Min Ye*

State Key Laboratory of Natural and Biomimetic Drugs, School of Pharmaceutical Sciences, Peking University, 38 Xueyuan Road, Beijing 100191, China
* Corresponding authors, E-mail: qiaoxue@bjmu.edu.cn; yemin@bjmu.edu.cn

Abstract

C-glycosides are an important class of bioactive natural products, and the *C*-glycosidic bonds are usually catalyzed by *C*-glycosyltransferases. In this work, an efficient and rare CGT, LaCGT1, was discovered from the aquatic plant *Lemna aequinoctialis*. LaCGT1 could accept five sugar donors (UDP-Glc/-Xyl/-Gal/-GlcNAc/-Ara) to catalyze *C*-glycosylation, and showed strong preference to uridine 5′-diphosphate xylose (UDP-Xyl). LaCGT1 catalyzed at least six substrates using UDP-Xyl as sugar donor, with conversion rates of > 95%. Three xylosides were obtained by scaled-up enzymatic catalysis, and their structures were identified by 1D NMR, 2D NMR, and HR-ESIMS data analyses. Molecular modeling and site-directed mutagenesis indicated that R271, W357, D378, and Q379 residues were key amino acids contributing to sugar donor recognition of UDP-Xyl. LaCGT1 could be a promising catalyst to prepare bioactive flavonoid *C*-xylosides.

Citation: Shaker S, Hu Z, Wang Z, Ye G, Long J, et al. 2022. Functional characterization of a UDP-xylose-preferring *C*-glycosyltransferase from *Lemna aequinoctialis*. *Medicinal Plant Biology* 1:2 https://doi.org/10.48130/MPB-2022-0002

INTRODUCTION

In plants, *C*-glycosylation is catalyzed by *C*-glycosyltransferases (CGTs). These enzymes could condense an activated sugar moiety (for instance, UDP-sugar) with an acceptor molecule (for instance, a 2-hydroxyflavanone or a flavonoid) to produce diverse *C*-glycosylated natural products (*C*-glycosides). The *C*-glycosidic linkage has strong stability against gastrointestinal hydrolysis metabolism[1]. Accordingly, *C*-glycosides exhibit remarkable bioactivities, and the sugar moieties contribute to their structural diversity and bioactivity. For instance, apigenin 6,8-di-*C*-β-D-xylopyranoside showed strong anti-inflammatory activities by reducing TNF-α and NO[2]. *C*-β-D-xylopyranoside-2-hydroxy-propane could enhance epithelial repair by serving as an initiator of Dermatan sulfate (DS) synthesis[3]. Vicenin-2 (apigenin 6,8-di-*C*-glucoside) could inhibit diabetic vascular inflammation[4]. Besides, aspalathin, a dihydrochalcone *C*-glucoside, exhibits beneficial effects on glucose homeostasis in type II diabetes through stimulating glucose uptake in muscle tissues and insulin secretion from pancreatic β-cells and thus could potentially be used to treat diabetes[5]. Furthermore, (iso)schaftosides (containing glucose and arabinose residues at C-6 and C-8) are important plant defense compounds, and their production is related with drought tolerance of wheat leaves and ultraviolet resistance of rice seeds[6].

Thus far, around 70 CGTs have been characterized from plants (Supplemental Fig. S1)[7]. They exhibit promiscuous selectivity for sugar donors, and most of them could accept uridine 5′-diphosphate glucose (UDP-Glc), including GgCGT[8], TcCGT1[9], MiCGT[10], FeCGTa[11], SbCGTa[12] and SbCGTb, though it shows obvious preference order. For instance, GgCGT showed the preference order of UDP-Glc > UDP-Xyl > UDP-Gal > UDP-Ara. SbCGTb showed the preference order of UDP-Ara > UDP-Xyl > UDP-Glc. These CGTs could not highly convert substrates to *C*-xylosides when the content of enzyme is low. However, no CGTs with high preference to UDP-Xyl have been reported, thus far. In this work, we report an efficient *C*-glycosyltransferase, LaCGT1, from the aquatic plant *Lemna aequinoctialis*. LaCGT1 showed remarkable preference to UDP-Xyl and could catalyze at least six substrates with high conversion rates (> 95%).

RESULTS

Molecular cloning and functional characterization of LaCGT1

Lemna aequinoctialis is a tiny aquatic plant (monocotyledonous) widely distributed in tropical and subtropical regions (Supplemental Fig. S2). It contains abundant *C*-glycosides including (iso)schaftosides and (iso)vitexins[13]. Thus, we mined the transcriptome data (SRR5688503, and SRR5688504) of *L. aequinoctialis*. A total of 11 known plant CGT genes were used as templates in BLAST search and the cutoff e-value was set as $1e^{-41}$. Finally, five putative genes with open reading frames (ORF) were screened out. Among them, LaCGT1 was tentatively identified as *C*-glycosyltransferases according to the PSPG box and DPF conservative motif (Supplemental Fig. S3). LaCGT1 (UGT708P3, Accession number: ON165544) contains a 1383-bp ORF encoding 460 amino acid polypeptides. The coding region was cloned into pET-32a(+) vector and the protein was expressed in an *E. coli* BL21(DE3) strain. The recombinant protein was purified by Ni-NTA affinity chromatography (Supplemental Fig. S4).

The function of LaCGT1 was characterized by coincubating 20 μg purified protein, 0.1 mM phloretin (**1**) and 0.5 mM UDP-glucose (UDP-Glc) in 100 μL of 50 mM PBS (Na_2HPO_4-NaH_2PO_4)

buffer (pH 8.0, 25 °C, 2 h). As shown in Supplemental Fig. S5, at the presence of UDP-Glc, LaCGT1 could completely convert **1** into **1b**, and could partially convert **1b** into a more polar product **1c**. The mass spectrum of **1b** showed an $[M-H]^-$ ion at *m/z* 434.9, which could produce fragments at *m/z* 314.9 ($[M-H-120]^-$), indicating **1b** as a mono-*C*-glucoside. The product **1c** showed an $[M-H]^-$ ion at *m/z* 597.1, which could produce fragments at *m/z* 477.1 ($[M-H-120]^-$) and *m/z* 357.1 ($[M-H-240]^-$), indicating **1c** as a di-*C*-glucoside. Interestingly, LaCGT1 also showed preference to UDP-Xyl. With the presence of UDP-Xyl, LaCGT1 could completely convert **1** into one single glycosylated product **1a**. The mass spectrum of **1a** showed an $[M-H]^-$ ion at *m/z* 405.0 (Fig. 1a–c), which could produce fragments at *m/z* 345.2 ($[M-H-60]^-$), and *m/z* 315.3 ($[M-H-90]^-$), indicating **1a** as *C*-xylosyl phloretin. The product **1a** was subsequently prepared via a preparative-scale reaction for structural characterization. The heteronuclear multiple bond correlation (HMBC) spectrum of **1a** showed a long-range correlation from H-1″ (δ_H 4.74) to C-3′ (δ_C 104.1), indicating the sugar moiety was linked to C-3′ (Fig. 1d). Thus, **1a** was identified as phloretin 3′-*C*-β-D-xyloside. Then we tested the effects of reaction temperature, reaction time, reaction buffer, and divalent metal ions on the activities of LaCGT1. Phloretin (**1**) was used as the acceptor and UDP-Xyl as the sugar donor, and an optimized reaction time of 60 min was used. LaCGT1 exhibited its maximum activity at pH 8.0 (50 mM Na_2HPO_4-NaH_2PO_4) and 25 °C (Supplemental Fig. S6). Then, we measured the K_m and k_{cat}/K_m values (catalytic efficiency) for LaCGT1 with phloretin. The K_m was 23.4 μM, k_{cat}/K_m value was 0.0399 μM^{-1} s^{-1} (Supplemental Fig. S7).

Substrate specificity of LaCGT1

To explore the substrate specificity and promiscuity of LaCGT1, seven substrates and 17 compounds of different types were tested using UDP-Xyl as sugar donor (Fig. 2, Supplemental Fig. S8). The reaction mixtures were analyzed by liquid chromatography coupled with mass spectrometry (LC/MS) (Supplemental Fig. S9–S15). LaCGT1 showed high conversion rates (> 95%) for **2**–**6**, and a relatively low conversion rate (> 40%) for **7**. LaCGT1 could catalyze substrates with a 2′,4′,6′-trihydroxyacetophenone unit. These results indicated 2′,4′,6′-trihydroxyacetophenone as the minimum unit required for *C*-xylosylation of LaCGT1. In the meantime, substrate binding region of LaCGT1 could recognize 2′,4′,6′-trihydroxyacetophenone as minimum unit, otherwise the substrate could not be stable in the active pocket and the *C*-xylosylation could not happen. Among them, **1a**, **5a** and **6a** were purified by scaled-up enzymatic reactions, and their structures were unambiguously identified by NMR spectroscopic analyses (Table 1, Supplemental Fig. S16–S23)[8]. The other types of substrates could not be recognized by LaCGT1.

Sugar donor preference of LaCGT1

To further explore the sugar donor preference of LaCGT1, five other sugar donors were tested, i.e., UDP-Glc, UDP-Ara, UDP-Gal, UDP-GlcNAc, and UDP-GlcA. When phloretin (**1**) was used as the substrate, LaCGT1 could utilize all the donors except from UDP-GlcA to generate *C*-glycosides at high enzyme concentrations. Their products were characterized by LC/MS (Supplemental Fig. S5). When the protein amount was reduced to 10 μg and the reaction time was reduced to 30 min, LaCGT1 showed the preference order of UDP-Xyl > UDP-Glc > UDP-GlcNAc > UDP-Gal > UDP-Ara (Fig. 3). This result indicated significance of the stereo-configuration (α or β) of sugar 4-OH in catalytic efficiency, which is consistent with our previous report[8].

Molecular modeling study

To further investigate mechanisms for the sugar donor selectivity of LaCGT1, molecular modeling was conducted. The

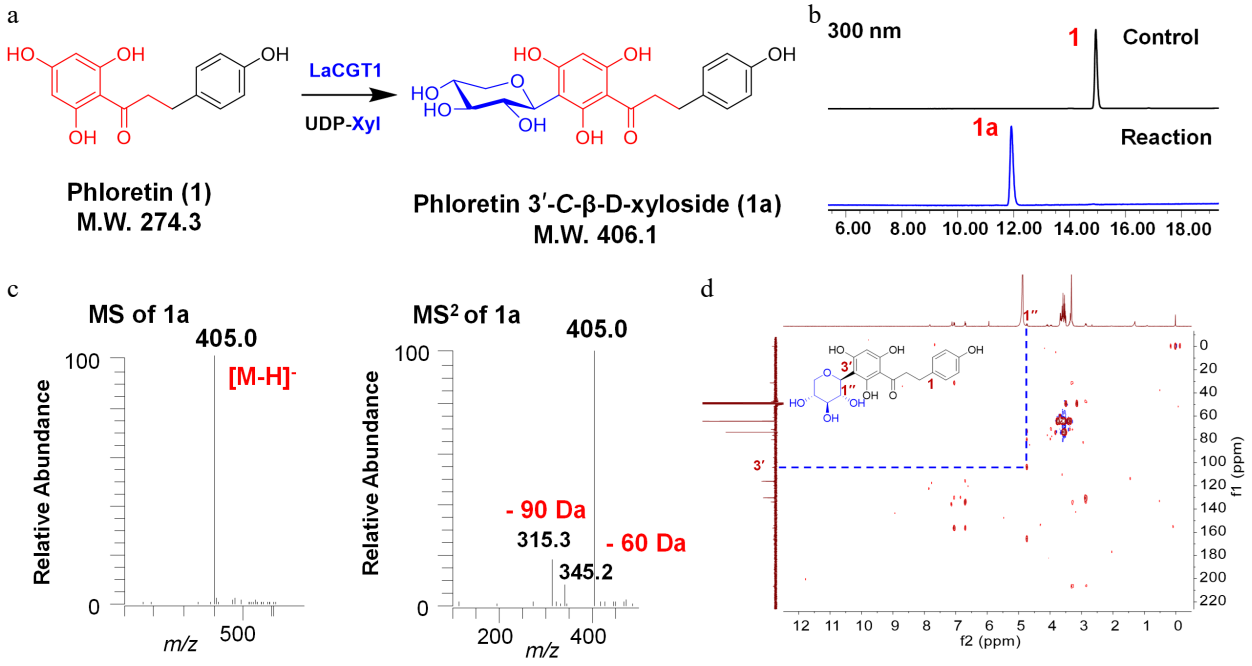

Fig. 1 *C*-xylosylation of phloretin (**1**) by LaCGT1. (a) Glycosylation of **1** by recombinant LaCGT1 to produce **1a** using UDP-Xyl as sugar donor. (b) HPLC chromatograms of the enzymatic reaction mixture and the control. (c) LC/MS analysis of **1a** in the negative ion mode. (d) HMBC spectrum of **1a** (methanol-d_4, 400 MHz).

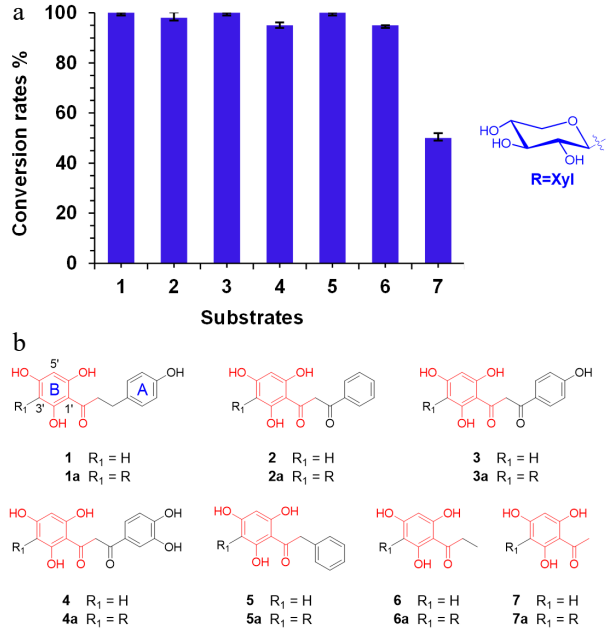

Fig. 2 Substrate specificity of LaCGT1. (a) Conversion rates (%) of glycosylated products for substrates **1–7**, using UDP-Xyl as the sugar donor. The conversion rates were calculated by HPLC peak area ratio and the experiments were performed in triplicate. (b) Structures of **1–7**.

Table 1. ^{1}H NMR data of compounds **1a**, **5a**, and **6a** (δ in ppm, J in Hz, measured at 400 MHz in methanol-d_4).

Position	δ_H of **1a**	δ_H of **5a**	δ_H of **6a**
Aglycone:			
1			
2	7.06 (2H, d, J = 8.4 Hz)	4.31 (2H, m)	
3	6.70 (2H, d, J = 8.4 Hz)		
4			
5	6.70 (2H, d, J = 8.4 Hz)	5.92 (1H, s)	5.92 (1H, s)
6	7.06 (2H, d, J = 8.4 Hz)		
α	3.36 (2H, m)		3.08 (2H, d, J = 7.3 Hz)
β	2.86 (2H, m)		1.13 (3H, t, J = 7.3 Hz)
1′			
2′		7.18 (2H, m)	
3′	2.00, 1.49	7.09 (2H, m)	
4′		7.20 (2H, m)	
5′	5.95 (1H, s)	5.85 (1H, s)	
6′			
Xylosyl:			
1	4.74 (1H, d, J = 9.9 Hz)	4.65 (1H, d, J = 9.9 Hz)	4.72 (1H, d, J = 9.9 Hz)
2	4.09 (1H, t, J = 9.3 Hz)	4.00 (1H, t, J = 9.2 Hz)	4.05 (1H, t, J = 9.1 Hz)
3	3.38 (1H, m)	3.34 (1H, m)	3.37 (1H, m)
4	3.68 (1H, m)	3.55 (1H, m)	3.63 (1H, m)
5	3.97 (1H, m, H-a); 3.28 (1H, m, H-b)	3.88 (1H, t, J = 5.5 Hz); 3.19 (1H, m)	3.96 (m, H-a); 3.25 (m, H-b)

protein model for LaCGT1 was established by homologous molecular modeling using SWISS-MODEL[14]. The crystal structure of GgCGT with UDP-Glc (PDB ID:6L5P), which exhibits reliability with a GMQE (global model quality estimation) value of 0.73, was used as the modeling template. It shares amino acid sequence identity of 45.83% with LaCGT1, with root-mean-square deviation (RMSD) of < 1.4 Å for the backbone.

We simulated UDP-Xyl to the LaCGT1 model according to reported complex structures (Fig. 4a). The simulated struture of LaCGT1/UDP-Xyl indicated that 2-OH, 3-OH, and 4-OH of the xylosyl moiety could form hydrogen bonds with R271, W357, D378, and Q379. Particularly, the residues of D378 and Q379 could interact with 2-OH (one interaction), 3-OH (two interactions), and 4-OH (one interaction) through four hydrogen bonds. In addition, the nitrogen atoms of R271 and W357 could also interact with 2-OH (one interaction), and 4-OH (one interaction), respectively (Fig. 4b). Thus, we constructed mutants R271A, W357A, D378A, and Q379A. All the mutants showed virtually no catalytic activities, indicating R271, W357, D378 and Q379 as key amino acids contributing to sugar donor recognition of UDP-Xyl (Fig. 4c, d).

DISCUSSION

LaCGT1 showed preference to UDP-xylose, which is remarkably different from previously reported CGTs in sugar donor selectivity. Our experiments indicated that R271, W357, D378 and Q379 in LaCGT1 could be key amino acids for the selectivity. However, these residues are highly conserved in almost all CGTs by sequence alignment (Supplemental Fig. S3). Thus, we specluate that other key amino acids remain undiscovered to determine the recognition and preference of UDP-Xyl. In our previous studies, we have reported a series of *O*-glycosyltransferases with high sugar donor selectivity, including rhamnosyltransferase[15], arabinosyltransferase[12], and galactosyltransferase[16]. The detailed mechanisms for sugar donor selectivity of glycosyltransferases require further study.

CONCLUSIONS

In conclusion, we cloned and characterized a *C*-glycosyltransferase, LaCGT1, from the aquatic plant *Lemna aequinoctialis*. LaCGT1 could efficiently catalyze *C*-glycosylation of at least six substrates with high conversion rates (> 95%) using UDP-xylose as sugar donor. The products **1a** (phloretin 3′-*C*-*β*-D-xyloside), **5a** (2-phenyl-3′-(*C*-*β*-D-xylosyl)-2′,4′,6′-trihydroxyacetophenone), and **6a** (flopropione 3′-*C*-*β*-D-xyloside) were prepared from preparative-scale reactions for structural characterization, and **1a** and **6a** are new compounds. LaCGT1 showed unprecedented sugar donor preference of UDP-Xyl > UDP-Glc > UDP-GlcNAc > UDP-Gal > UDP-Ara. Molecular docking and site-directed mutagenesis indicated that R271, W357, D378 and Q379 may play a significant role in donor preference. LaCGT1 is a promising catalyst to prepare flavonoid *C*-xylosides.

MATERIALS AND METHODS

Materials

Substrates **1**–**18**, **21–24** were purchased from Chengdu Gelaite Biological Technology Co., Ltd, Chengdu Must Biotechnology Co., Ltd and Chengdu Push Biotechnology Co., Ltd (Chengdu, China). Compounds (**19–20**) were synthesized as previously described[12]. Methanol and acetonitrile (Fisher Scientific, USA) were of HPLC grade. All other chemicals and

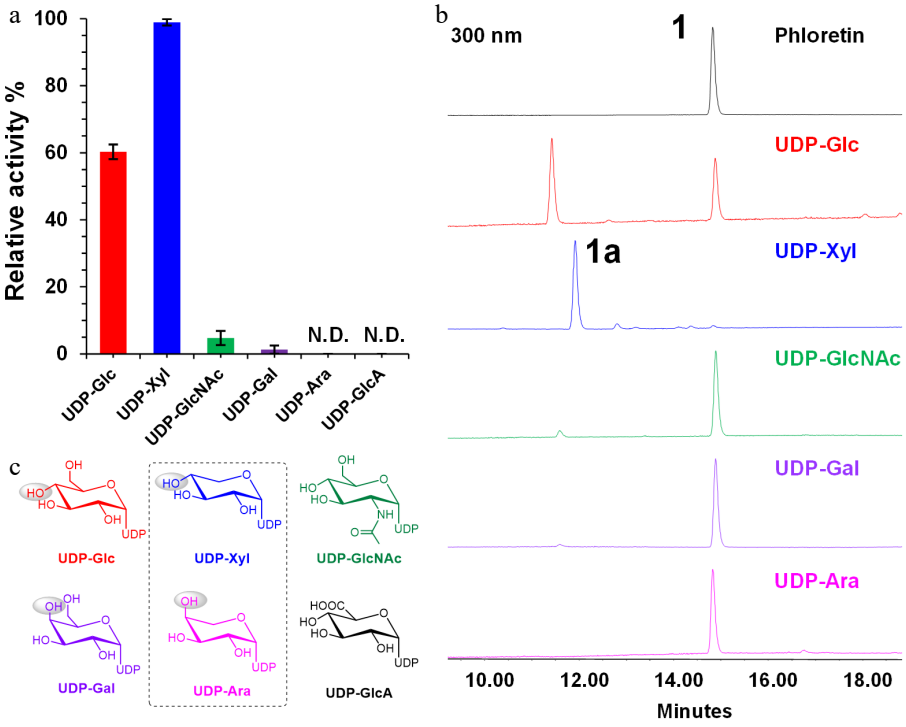

Fig. 3 Sugar donor preference of LaCGT1 at low enzyme concentration. (a) Relative conversion rates of *C*-glycosylated products using different sugar donors. The experiments were performed in triplicate. (b) HPLC chromatograms of enzyme reactions of LaCGT1 with different sugar donors at low enzyme concentration. (c) Structures of sugar donors.

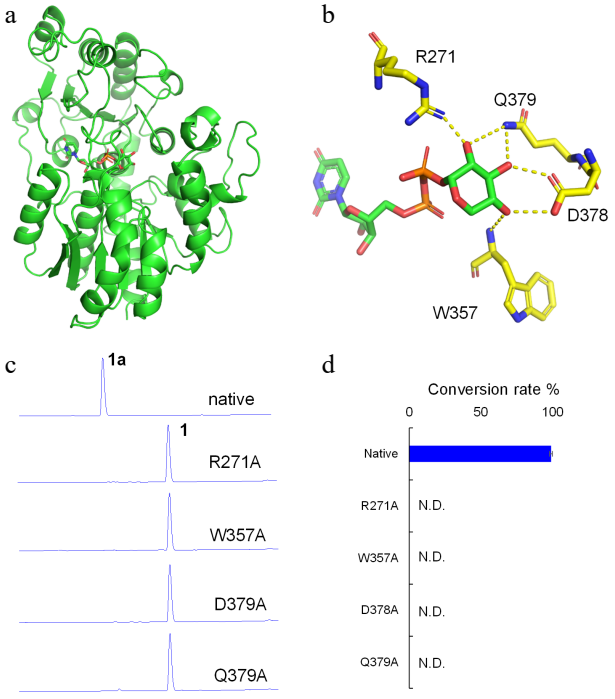

Fig. 4 Molecular modeling and site-directed mutagenesis for LaCGT1. (a) The model of LaCGT1/UDP-Xyl. (b) Key amino acid residues around the xylose residue of UDP-Xyl in LaCGT1. The hydrogen-bond interactions are shown as yellow dashes. (c, d) The glycosylation conversion rates of native and mutants, using phloretin (**1**) and UDP-Xyl as the sugar acceptor and donor, respectively. The reaction mixtures were incubated at 25 °C for 1 h. Molecular docking was carried out by Autodock and the results were visualized using AutoDocktools v1.5.6 and Pymol. N.D., not detected.

reagents were purchased from Sigma-Aldrich (St. Louis, MO, USA) and Beijing Chemical Corporation (Beijing, China) unless otherwise specified. The glycosylated products and conversion rates were analyzed by HPLC on an Agilent 1260 instrument (Agilent Technologies, Waldbronn, Germany) and a Waters 2695 HPLC instrument (Waters Technologies, Massachusetts, USA). LC-MS analysis was performed on an LCQ Advantage ion-trap mass spectrometer (Thermo Fisher, CA, USA) and A Thermo UHPLC instrument was coupled with a Q-Exactive hybrid quadrupole-Orbitrap mass spectrometer through a heated ESI source (Thermo Fisher Scientific, CA, USA). ESI source parameters: negative ion polarity mode; sheath gas (N_2), 50 arb; auxiliary gas (N_2), 10 arb; spray voltage, 4.5 kV; capillary temperature, 330 °C; collision energy, −10 V; normalized collision energy, 38%. NMR spectra were recorded on a Bruker AVANCE III-400 instrument at 400 MHz for ^{1}H and 100 MHz for ^{13}C in methanol-d_4, using TMS as reference. *Lemna aequinoctialis* Welwitsch was obtained from Jinhua (Zhejiang, China) and was immediately frozen in liquid nitrogen for RNA extraction. The photo of fresh plant material of *Lemna aequinoctialis* and RNA electrophoresis are shown in Supplemental Fig. S2.

Transcriptome data assembly and candidate gene screening

Seed transcriptome data of *Lemna aequinoctialis* Welwitsch (SRR5688502, and SRR5688503) were downloaded from NCBI (www.ncbi.nlm.nih.gov), and were assembled through the SOAPdenovo-Trans-src-v1.04 program (Supplemental Table S2). For BLAST analysis, *C*-glycosyltransferases MiCGT[10], MiCGTb[17], UGT708D1[18], FeCGTa[11], FeCGTb[11], OsCGT[19], UGT708A6[20], PlUGT43[21], GtUF6CGT1[22], FcCGT[23], and CuCGT[23] were used as query sequences. LaCGT1 was discovered according to the PSPG box and DPF conservative

motifs of *C*-glycosyltransferases. LaCGT1 was cloned, and the PCR primers containing the homologous sequences of pET-32a(+) are shown in Supplemental Table S1.

RNA extraction, molecular cloning, heterologous expression, and protein purification

The total RNA of *Lemna aequinoctialis* Welwitsch was extracted from the frozen whole plant by grinding seedlings with a mortar and pestle under liquid nitrogen using TransZol method in accordance with the manufacturer's instructions (Transgen Biotech, Beijing, China). First-strand cDNA was synthesized from the total RNA using SMART RACE cDNA Amplification Kit (Clontech Laboratories, Inc., California, USA). PCR was performed using 2 μl of cDNA as a template, LaCGT1-F and LaCGT1-R as primers, and KD Plus DNA polymerase under the following conditions: 94 °C for 3 min, 35 cycles of 94 °C for 30 s, 60 °C for 30 s, 68 °C for 1.5 min, followed by 68 °C for 10 min. The amplified fragments were cloned into pET-32a(+) vector (Invitrogen, California, USA) by Quick-change method. The gene was sequenced by Tsingke Biological Technology (Beijing, China). The recombinant vector pET-32a(+)-LaCGT1 was transformed into *E. coli* BL21(DE3) (TransGen Biotech, Beijing, China) for heterologous expression. Transformed cells were selected on agar plates containing 100 μg/ml ampicillin.

Single colonies harboring the desired expression construct were inoculated overnight at 37 °C with shaking in LB culture medium containing 100 μg/ml ampicillin. Isopropyl thiogalactoside (0.1 mM) was added into the medium for the expression of recombinant protein at 18 °C when optical density at 600 nm was 0.6–0.8. After incubating with shaking for 20 h, *E. coli* were harvested by centrifugation. The recombinant protein was purified using a nickel-affinity column (*Proteinlso* Ni-NTA Resin, TransGen Biotech, Beijing, China), and concentrated using Amicon Ultra-15 Ultracel-30K (Merck Millipore). The concentrated protein was used as purified recombinant enzymes. The recombinant LaCGT1 analyzed by SDS-PAGE is shown in Supplemental Fig. S4. The concentration of recombinant enzyme was determined according to enhanced BCA protein assay kit (Beyotime Institute of Biotechnology, Shanghai, China).

Effects of reaction time, pH, temperature, and divalent metal ion

To characterize the enzymatic properties of LaCGT1, its optimum reaction time, pH, temperature and divalent metal ions were studied. To investigate the reaction time, 11 time points between 5 min and 300 min were studied. To optimize the reaction pH, the enzymatic reactions were carried out in various reaction buffers ranging in pH values from 5.0–6.0 (Citric acid-sodium citrate buffer), 6.0–9.0 (Na_2HPO_4-NaH_2PO_4 buffer), 7.0–9.0 (Tris-HCl buffer), and 9.0–10.0 (Na_2CO_3-$NaHCO_3$ buffer). To investigate the optimal reaction temperature, the enzymatic reactions were incubated at different temperatures (4–60 °C). To test the dependence of divalent metal ions for LaCGT1 activity, different divalent cations Ba^{2+}, Ca^{2+}, Zn^{2+}, Mg^{2+}, Mn^{2+}, Ni^{2+}, Fe^{2+}, Cu^{2+}, EDTA and blank in the final concentration of 5 mM were used, individually. All enzymatic reactions were conducted with UDP-Xyl as a donor and phloretin (**1**) as an acceptor. All experiments were performed in triplicate and the mean value was used. All the reactions were terminated with pre-cooled methanol and centrifuged at 15,000 rpm for 15 min for HPLC analysis as described in general methods. The samples were analyzed by an Agilent Zorbax SB C_{18} column (250 mm × 4.6 mm, 5 μm) at a flow rate of 1 mL min^{-1}. The column temperature was 25 °C and the enzymatic products were eluted with a linear gradient of 20%–100% methanol in H_2O containing 0.1% formic acid in 20 min, followed by 100% methanol for 5 min. The conversion rates in percentage were calculated from peak areas of glycosylated products and substrate.

In vitro enzyme catalytic activity assay

To investigate the substrate promiscuity and specificity of LaCGT1, different acceptors including compounds **1–24** (Supplemental Figs. S3, S8) were used. The reaction mixtures were individually performed in a final volume of 100 μL containing 50 mM PBS buffer (pH 8.0), 20 μg of purified LaCGT1, 0.1 mM aglycone, and 0.5 mM sugar-donor. All reactions were incubated at 25 °C for 1 h and quenched with 100 μL ice cold methanol. The mixtures were then centrifuged at 15,000 rpm for 15 min and analyzed by LC/MS. The HPLC mobile phase consisted of methanol (A) and water containing 0.1% formic acid (*v/v*, B). The analytes were eluted using a linear gradient program: 0–20 min, 20%–100% A; 20–25 min, 100% A; 26–31 min, 20% A. The flow rate was 1 mL/min. The column temperature was 25 °C. The detection wavelength was 300 nm.

Site-directed mutagenesis

The mutants of LaCGT1 were obtained by Fast Mutagenesis system (Transgen Biotech, Beijing, China). The positive recombinant plasmids were transformed into *E. coli* BL21(DE3) for heterologous expression. The other conditions were the same as described above.

Kinetic studies

For kinetic studies of LaCGT1, enzymatic assays were performed in a final volume of 50 μL containing 50 mM Na_2HPO_4-NaH_2PO_4 buffer (pH 8.0), 0.2 μg of purified LaCGT1, 2 mM of saturated UDP-Xyl, and varying concentrations (5–120 μM) of phloretin (**1**). The reactions were conducted at 25 °C for 10 min and then quenched with 100 μL ice cold methanol. Samples were centrifuged at 15,000 rpm for 15 min and analyzed by HPLC as described above. All experiments were performed in triplicate. The Michaelis-Menten plot was fitted (Supplemental Fig. S7).

Preparative-scale purification of glycosylated products

The aglycones (10 mg for **1** and **5**; 5 mg for **6**) were dissolved in dimethyl sulfoxide (DMSO) at a concentration of 25 mM and then diluted with reaction buffer (50 mM Tris-HCl, pH 8.0) to a final concentration of 1 mM. Two-fold UDP-Xyl was added along with purified glycosyltransferases (5 mg protein per mg substrate). The reactions were incubated overnight at 25 °C and terminated with methanol. The mixtures were then centrifuged at 15,000 rpm for 30 min and the supernatants were concentrated and dissolved in 50% methanol. The samples were then purified by semi-preparative HPLC on an Agilent 1200 instrument equipped with an Agilent Zorbax SB C_{18} column (9.4 × 250 mm, 5 μm).

ACKNOWLEDGMENTS

This work was supported by the National Natural Science Foundation of China (Grant No. 81725023, 82122073), and the National Key Research and Development Program of China (No. 2017YFC1700405).

Conflict of interest

The authors declare that they have no conflict of interest.

Supplementary Information accompanies this paper at (http://www.maxapress.com/article/doi/10.48130/MPB-2022-0002)

Dates

Received 9 February 2022; Accepted 5 May 2022; Published online 23 May 2022

REFERENCES

1. Williams GJ, Zhang C, Thorson JS. 2007. Expanding the promiscuity of a natural-product glycosyltransferase by directed evolution. *Nature Chemical Biology* 3:657–662
2. Shie JJ, Chen CA, Lin CC, Ku AF, Cheng TJ, et al. 2010. Regioselective synthesis of di-*C*-glycosylflavones possessing anti-inflammation activities. *Organic & Biomolecular Chemistry* 8:4451–62
3. Muto J, Naidu NN, Yamasaki K, Pineau N, Breton L, et al. 2011. Exogenous addition of a *C*-xylopyranoside derivative stimulates keratinocyte dermatan sulfate synthesis and promotes migration. *PLoS One* 6:e25480
4. Ku SK, Bae JS. 2016. Vicenin-2 and scolymoside inhibit high-glucose-induced vascular inflammation in vitro and *in vivo*. *Canadian Journal of Physiology and Pharmacology* 94:287–95
5. Han Z, Achilonu MC, Kendrekar PS, Joubert E, Ferreira D, et al. 2014. Concise and scalable synthesis of aspalathin, a powerful plasma sugar-lowering natural product. *Journal of Natural Products* 77:583–88
6. Galland M, Boutet-Mercey S, Lounifi I, Godin B, Balzergue S, et al. 2014. Compartmentation and dynamics of flavone metabolism in dry and germinated rice seeds. *Plant and Cell Physiology* 55:1646–59
7. Putkaradze N, Teze D, Fredslund F, Welner DH. 2021. Natural product *C*-glycosyltransferases - a scarcely characterised enzymatic activity with biotechnological potential. *Natural Product Reports* 38:432–43
8. Zhang M, Li F, Li K, Wang Z, Wang Y, et al. 2020. Functional characterization and structural basis of an efficient di-*C*-glycosyltransferase from *Glycyrrhiza glabra*. *Journal of the American Chemical Society* 142:3506–12
9. He J, Zhao P, Hu Z, Liu S, Kuang Y, et al. 2019. Molecular and structural characterization of a promiscuous *C*-glycosyltransferase from *Trollius chinensis*. *Angewandte Chemie* 58:11513–20
10. Chen D, Chen R, Wang R, Li J, Xie K, et al. 2015. Probing the catalytic promiscuity of a regio- and stereospecific *C*-glycosyltransferase from *Mangifera indica*. *Angewandte Chemie* 54:12678–82
11. Nagatomo Y, Usui S, Ito T, Kato A, Shimosaka M, Taguchi G. 2014. Purification, molecular cloning and functional characterization of flavonoid *C*-glucosyltransferases from *Fagopyrum esculentum* M. (buckwheat) cotyledon. *The Plant Journal* 80:437–48
12. Wang Z, Gao H, Wang S, Zhang M, Chen K, et al. 2020. Dissection of the general two-step di-*C*-glycosylation pathway for the biosynthesis of (iso)schaftosides in higher plants. *PNAS* 117:30816–23
13. Yoshida A, Taoka KI, Hosaka A, Tanaka K, Kobayashi H, et al. 2021. Characterization of frond and flower development and identification of FT and FD genes from duckweed *Lemna aequinoctialis* Nd. *Frontiers in Plant Science* 12:697206
14. Biasini M, Bienert S, Waterhouse A, Arnold K, Studer G, et al. 2014. SWISS-MODEL: modelling protein tertiary and quaternary structure using evolutionary information. *Nucleic Acids Research* 42:W252–W258
15. Liu S, Zhang M, Bao Y, Chen K, Xu L, et al. 2022. Characterization of a highly selective 2''-*O*-galactosyltransferase from *Trollius chinensis* and structure-guided engineering for improving UDP-glucose selectivity. *Organic Letters* 23:9020–9024
16. Wang Z, Zhou J, Han B, Hasan A, Zhang Y, et al. 2022. GuRhaGT, a highly specific saponin 2''-*O*-rhamnosyltransferase from *Glycyrrhiza uralensis*. *Chemical Communications* 58:5277–80
17. Chen D, Fan S, Chen R, Xie K, Yin S, et al. 2018. Probing and engineering key residues for bis-*C*-glycosylation and promiscuity of a *C*-glycosyltransferase. *ACS Catalysis* 8:4917–27
18. Hirade Y, Kotoku N, Terasaka K, Saijo-Hamano Y, Fukumoto A, Mizukami H. 2015. Identification and functional analysis of 2-hydroxyflavanone *C*-glucosyltransferase in soybean (*Glycine max*). *FEBS Letters* 589:1778–86
19. Hao B, Caulfield JC, Hamilton ML, Pickett JA, Midega CAO, et al. 2016. Biosynthesis of natural and novel *C*-glycosylflavones utilising recombinant *Oryza sativa C*-glycosyltransferase (OsCGT) and *Desmodium incanum* root proteins. *Phytochemistry* 125:73–87
20. Falcone Ferreyra ML, Rodriguez E, Casas MI, Labadie G, Grotewold E, et al. 2013. Identification of a bifunctional maize *C*- and *O*-glucosyltransferase. *Journal of Biological Chemistry* 288:31678–88
21. Wang X, Li C, Zhou C, Li J, Zhang Y. 2017. Molecular characterization of the *C*-glucosylation for puerarin biosynthesis in *Pueraria lobata*. *The Plant Journal* 90:535–46
22. Sasaki N, Nishizaki Y, Yamada E, Tatsuzawa F, Nakatsuka T, et al. 2015. Identification of the glucosyltransferase that mediates direct flavone *C*-glucosylation in *Gentiana triflora*. *FEBS Letters* 589:182–87
23. Ito T, Fujimoto S, Suito F, Shimosaka M, Taguchi G. 2017. *C*-glycosyltransferases catalyzing the formation of di-*C*-glucosyl flavonoids in citrus plants. *The Plant Journal* 91:187–98